

Design and Construction of Solid State Ag/AgCl Reference Electrodes Through Electrochemical Deposition of Ag and AgCl Onto a Graphite/Epoxy Resin-Based Composite. Parte 1: Electrochemical Deposition of Ag Onto a Graphite/Epoxy Resin-Based Composite

G. Valdés-Ramírez^{1,4}, M. T. Ramírez-Silva¹, M. Palomar-Pardavé^{2,*}, M. Romero-Romo², G. A. Álvarez-Romero³, P. R. Hernández-Rodríguez⁴, J.L. Marty⁵, J. M. Juárez-García⁶

¹ Universidad Autónoma Metropolitana–Iztapalapa, Departamento de Química. San Rafael Atlixco 186, Col. Vicentina, 09340 México, D. F. México

² Universidad Autónoma Metropolitana-Azcapotzalco, Departamento de Materiales, Av. San Pablo No. 180, Col. Reynosa, C.P. 02200 México D.F. México

³ Universidad Autónoma del Estado de Hidalgo. Centro de Investigaciones Químicas-Química Analítica. Unidad Universitaria, Carr. Pachuca-Tulancingo Km. 4.5, C.P. 42184 Mineral de la Reforma, Hidalgo, México.

⁴ CINVESTAV-Instituto Politécnico Nacional. Sección de Bioelectrónica. Depto. de Ing. Eléctrica. Av. IPN 2508, Col. Zacatenco. México D.F. México.

⁵ IMAGES EA4218, Centre de Phytopharmacie, Université de Perpignan Via Domitia, 52 avenue Paul Alduy, 66860 Perpignan Cedex, France

⁶ Centro Nacional de Metrología, Laboratorio de Microanálisis. km 4,5 de la Carretera a los Cues, municipio de El Marqués, Querétaro, México.

*E-mail: mepp@correo.azc.uam.mx

Received: 21 February 2011 / Accepted: 4 March 2011 / Published: 1 April 2011

In order to design and build solid state Ag/AgCl reference electrodes, the thick-film and thin-film techniques are frequently used to obtain a silver coating on a substrate that is subsequently chlorinated. In this part of the work we propose the use of a graphite/epoxy resin-based *composite* to electrodeposit silver onto its surface; to produce the said silver coating, we carried out potentiodynamic and potentiostatic studies of the silver electrodeposition process. The results obtained indicate a 3D silver nucleation and growth mechanism controlled by diffusion. Also it became apparent that obtaining a surface with variable roughness enables the deposition of up to a 100% more silver on the *composites* used. The present study has been carried out with the aim of obtaining design parameters to construct a silver coating reference solid state electrode as an alternative to thick and thin-film electrodes.

Keywords: Reference electrodes, silver, silver chloride, nucleation, composite

1. INTRODUCTION

Proper functioning of reference electrodes constitutes a basic requirement to any experimental electrochemical undertaking, although in particular, this is by and large a specific feature of reliable electrochemical analytical systems [1, 2]. Such systems have been and will continue to be an essential part of many researches [3-14]. As a matter of fact, the most commonly used reference electrodes have been: the saturated calomel electrode $\text{Hg}_{(l)}/\text{Hg}_2\text{Cl}_{2(s)}/\text{KCl}_{\text{sat}}$, the sulphate electrode $\text{Hg}_{(l)}/\text{HgSO}_{4(s)}/\text{K}_2\text{SO}_{4\text{sat}}$ and the silver chloride electrode $\text{Ag}_{(s)}/\text{AgCl}_{(s)}/\text{KCl}_{\text{sat}}$. However it is most likely in the latter case, this has been so because their more frequent use does not involve dangerously contaminating species as constituents of their electrochemical couple. These electrodes have allowed the possibility to obtain results during analyses of varied samples of interest to assorted industries as well as to research laboratories [1-15]. However, it is also truth that in some potentiometry analysis systems, non-Nernstian-type responses have been found occasionally, attributed to the liquid junction, common to conventional reference electrodes. Naturally, in order to solve this problem, one of the most viable strategies to eliminate the liquid junction through design and construction of reference electrodes without liquid junction, which entails the devises known either as solid state reference electrodes or pseudo-reference electrodes [3-14].

The design and manufacture of Ag/AgCl reference electrodes without liquid junction, have used very frequently the thick and thin-film technologies [3-14], aided by physical methods, such as screen-printing or Pulsed Laser Deposition (PLD). Plates of SiO_2 or Ti with silver layers are chlorinated subsequently, getting Ag/AgCl electrodes; even for microanalysis systems, solid state electrodes have been put to use but the cost involved turn them unaffordable [3-14]. Further, when considering that such electrodes may have short durability, attributed to low adherence among the materials employed and to the assembly form [3, 6-11], then the need to explore other materials capable of performing as adequate substrates to develop the solid state electrodes, becomes even stronger. Naturally, the use of other more traditional methods is not altogether excluded to obtain silver films on the substrates.

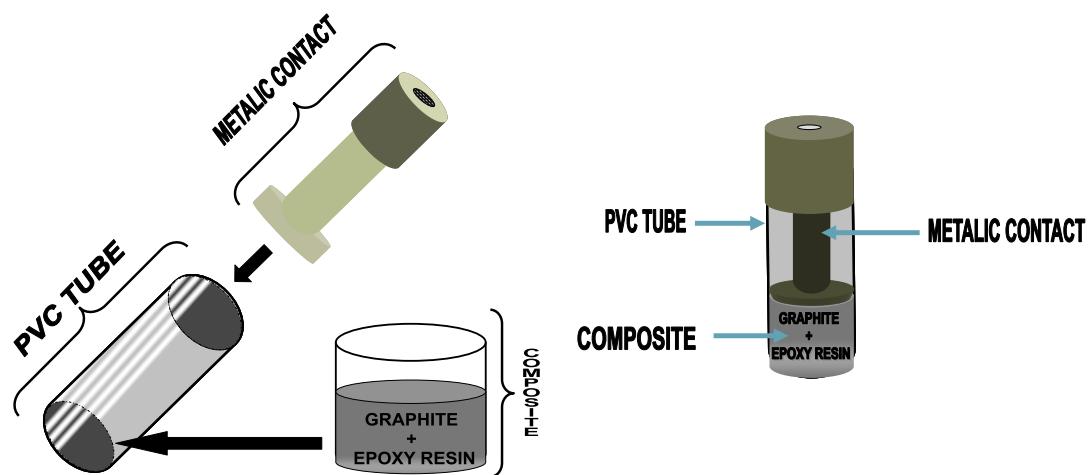
Numerous studies have been undertaken to attain metal films on various substrates, some of which have focussed on silver electrodeposition on substrates of carbon fibres, platinum microelectrodes, glassy carbon, copper wires and silicon plates, which have been mainly used to follow the electrodeposition process of the metal but also to modify the surface properties of the substrates employed [15-23]. Such studies have taken into consideration the environmental implications that are part of lixiviation processes of the mining industry [23]. Likewise silver electrodeposition is used in order to modify the electrical properties of materials used in the electronics industry [15]. Another application area of electrodeposition processes is in the design and construction of ion-selective electrodes, ISE, for Ag^+ , and to design affordable, reliable and environmentally friendly Ag/AgCl reference electrodes, with an appreciable durability and the inherent possibility to miniaturize them, so that they can be coupled to *in situ* surface characterization system as in Scanning Tunnelling Microscopy (STM) or, many batch potentiometric analysis systems, for instance.

Clearly, it would be of importance to fabricate reference electrodes with features such as those cited above. Therefore, this research work presents the results obtained through a comparative study on the potentiostatic and potentiodynamic silver electrodeposition processes onto a composite substrate (CE), made of a graphite-epoxy resin. The latter has been used also as membrane supports to construct sensors and as base material to disperse agents for biological recognition in the design and construction of sensors and biosensors [24-26]. The first part of the present paper shows the result of the study and optimization of the silver electrodeposition process onto the CE substrate. The second part of the research deals with the optimization of the electrochemical chlorination process of silver electrodeposits previously achieved onto the CE to form the CE/Ag_(s)/AgCl_(s), which is the construction base for solid state Ag_(s)/AgCl_(s) reference electrodes. Finally, the third part concerns the electrode's performance evaluation a reference electrode for ISE's electrodes for the analytic determination of several cations, namely Na⁺, NH₄⁺ and H⁺.

2. EXPERIMENTAL

2.1. Working electrodes

The composite electrodes (CE), were made from a mix of epoxy resin (Araldit HY, Ciba Geigy) with high purity powdered single crystal graphite (Alfa Aesar) in a 1:1 w/w ratio, poured into a PVC tube and subsequently fitted with a metal bar to serve as electric contact, as indicated in scheme 1. The CE was left to harden 60 hrs at constant 60 °C temperature.



Scheme 1. Fabrication of the composite electrode (CE).

2.2. CE surface finishings

In order to use the CE for silver electrodeposition, after consolidation of the composite, its exposed surface (scheme 1), was polished as follows: a) by preliminary metallographic grinding with

SiC paper down to 43 μm to form an electrode herein in this work as ECPL; b) subsequent to treatment a), the surface was polished with 1 μm alumina on a napless cloth, the polished electrode is named ECPA.

Either surface finish was used for separate experiments to gain further knowledge on their influence, as stated in the following section. The resulting electrodes displayed an electric resistance of $(11 \pm 3) \Omega$ and a geometrical surface area of $3.02 \times 10^{-5} \text{ m}^2$.

2.3. Equipment

A BAS W100 potentiostat was used to carry out all electrodepositions and the electrochemical studies ensuing, also with the aid of the typical three-electrode cell, which in this case had an ECPL or ECPA as working electrode, a Pt wire as auxiliary electrode and a sulphates electrode $\text{Hg}/\text{Hg}_2\text{SO}_4/\text{K}_2\text{SO}_{4\text{sat}}$, as reference for silver electrodeposition. Nitrogen was bubbled through the solution employed well before initiating the experiments in order to deareate them prior to any measurements. Also, the incidence of environmental illumination was precluded by covering the flasks with the electrolytes and/or analytes, to avoid any possible interactions.

2.4. Solutions

Silver was electrodeposited onto both ECPL and ECPA electrodes from an aqueous $2 \times 10^{-3} \text{ M}$ AgNO_3 containing 1 M KNO_3 at pH 5.98. The support electrolyte was prepared with the latter reagent grade salt supplied by Merck and deionized water with $18.2 \text{ M}\Omega\text{cm}$. To form AgCl , from the silver previously electrodeposited, an aqueous solution of KCl 0.1 M , pH= 6.85 was used.

2.5. Procedure

Cyclic voltammetry was used to find out the potential intervals in which the $\text{Ag}(\text{I})$ ion is reduced to $\text{Ag}(0)$ and the potential interval where oxidation of the electrodeposited silver takes place onto the ECPL and ECPA electrodes, using the three-electrode arrangement applying a single cycle program. Once the said potential intervals had been determined, a reduction potential range is selected to enable potentiodynamic and potentiostatic studies of silver electrodeposits, to determine the amount of silver deposited through each method cyclic voltammetry at oxidation range was applied. The silver deposition mechanism on the ECPL and ECPA was studied using chronopotentiometry.

The effect of the number of cycles and the potential scan rate on the amount of silver deposited on the composite was studied potentiodynamically, applying programs where the number of cycles was varied keeping constant the potential scan rate. After, the program giving the largest amount of silver is chosen to effect some variations to the scan rate in order to observe its outcome on the amount of deposit achieved.

The amount of silver deposited on the surface of each electrode is measured through the area under the anodic dissolution peak applying cyclic voltammetry, performed in the potential oxidation interval. This gives a clear indication of the amount of silver deposited on the composites.

In order to find out about the Ag(0) nucleation onto the composite substrate, potentiostatic studies were set up at different reduction potentials selected from the results of the characterization through CV done to know the response of the composites. The experimental results were compared with theoretical models [27-39] and, once the nucleation mechanism was identified, different potentials were selected and applied to the composite working electrode for varying times to observe the effect of these two parameters on the amount of silver electrodeposited, which was obtained in the same manner as indicated above in the potentiodynamic method.

3. RESULTS AND DISCUSSION

3.1. Voltammetry parameters for silver oxidation and reduction on the composite substrate.

Figure 1 shows typical voltammograms obtained when recording data within the reduction and oxidation potential intervals using the composite electrodes in the KNO₃ and AgNO₃ dissolution.

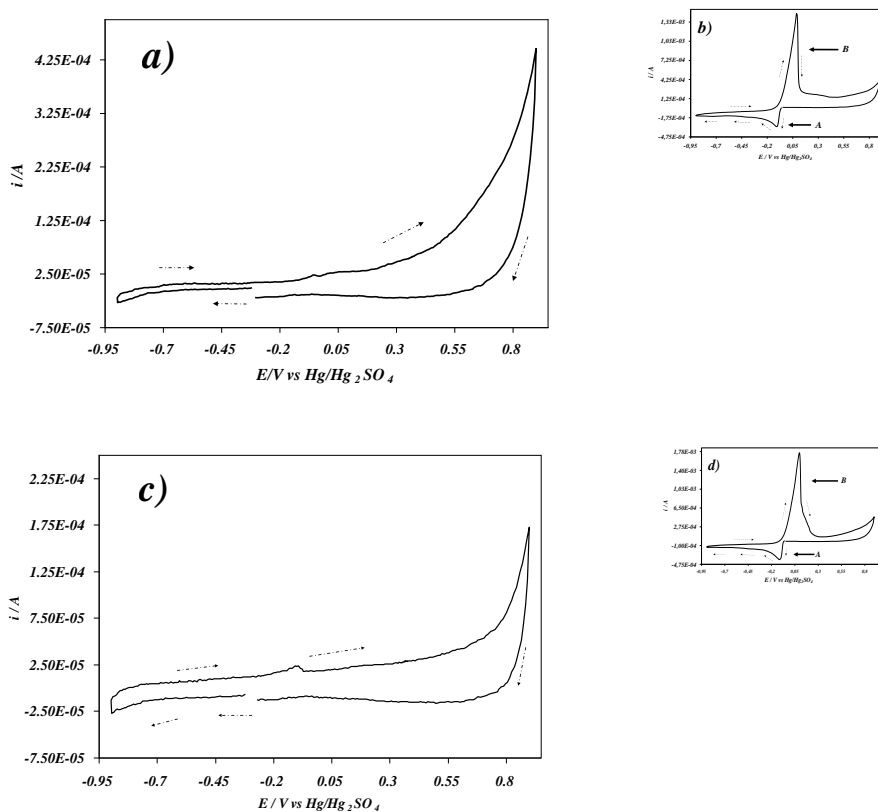


Figure 1. Typical voltammograms obtained at a potential scan rate of 0.100 Vs⁻¹ in the following systems: a) ECPL KNO₃ 1M, b) ECPL / KNO₃ 1M, AgNO₃ 2 mM, c) ECPA / KNO₃ 1M, d) ECPA / KNO₃ 1M AgNO₃ 2 mM. In all cases the potential scan started at the null current E_{i=0} in the cathodic direction.

For each case, the potential scan proceeded at a 0.100 V s^{-1} rate in the cathodic direction starting at the null current potential $E_{i=0}$

The voltammograms in Figure 1(a) and (c) shows that in the system studied with only the support electrolyte (KNO_3), there were no oxidation and reduction processes taking place within the potential interval studied; the null current potential was -0.350V for either of the electrodes ECPL and ECPA. Further, the voltammograms recorded in the presence of AgNO_3 , one peak **A** was observed associated to silver reduction given by: $\text{Ag}(I) + e^- \leftrightarrow \text{Ag}_{(s)}$. However, when reversing the direction of the scan the sharp peak appeared **B** associated to the oxidation of the silver metal deposited during reduction according to: $\text{Ag}_{(s)} \leftrightarrow \text{Ag}(I) + e^-$, see Figure 1 c) and d). The voltammetric characterization of both electrodes was done also in the presence of $\text{Ag}(I)$, as indicated by the results presented in Table 1.

Table 1. Voltammetry parameters obtained during $\text{Ag}(I)$ reduction and oxidation of silver metal deposited onto the composite electrodes finished to different surface roughness (ECPL and ECPA).

Electrode	$E_{i=0}/\text{V}$	E_{pc}/V	E_{pa}/V	i_{pc}/mA	i_{pa}/mA	$Q_{\text{anodic}}/Q_{\text{cathodic}}$
ECPL	-0.060	-0.125	0.095	-0.302	1.43	1.006
ECPA	-0.060	-0.130	0.100	-0.380	1.75	1.002

Table 1 shows that the null current potential was the same for both cases, however, the cathodic, E_{pc} , and the anodic peak potentials, E_{pa} , as well as the corresponding cathodic, i_{pc} , and anodic peak currents, i_{pa} , depend on the roughness of the substrate imparted during the aforementioned surface finishing procedure.

It can be observed that greater currents were obtained when the electrode was polished with alumina ECPA, which underlines at first that a larger amount of silver metal deposit is feasible on these composites, mainly attributed to a greater surface area available for development of nucleation and growth active sites, that resulted from the enforced mechanical development of a finer surface disposition of sites. Also, upon reversing the potential scan, all the silver deposited on the composite became oxidized as can be concluded from the ratio amount the anodic (Q_{anodic}) and cathodic (Q_{cathodic}) charges.

3.2. Potentiodynamic silver deposition study

Once the potential intervals for silver reduction and oxidation onto the ECPL and ECPA electrodes became known, a potential window from -0.080 to -0.500V was chosen for silver reduction

within which the electrodeposition studies were performed. In that same sense, the oxidation of the metal deposited previously was carried out in the -0.080 to 0.500 V, which was the potential range where electrodeposited silver became fully oxidized.

3.2.1. Effect of the cycle number on the amount of deposited silver

Silver electrodeposition was carried out in the -0.080 to -0.500 V applying 5, 10, 15 and 20 cycles at 0.100 Vs^{-1} for both types of surface rugosity, ECPL and ECPA.

After the silver deposition was completed, it was oxidized in the potential interval selected at the same potential scan rate; from the area under the oxidation peaks the corresponding charge was derived and subsequently, the amount of metal deposited. Table 2 shows the results obtained.

Table 2. Variation on the amount of silver electrodeposited as a function of the number of potential cycles within the reduction interval of -0.080 to -0.500 V at 0.100 Vs^{-1} .

Deposition number of cycles	ECPL		ECPA	
	Deposition time / s	Silver amount / nmoles	Deposition time / s	Silver amount / nmoles
5	44	9.1 ± 2.0	44	34.8 ± 1.7
10	88	16.5 ± 3.3	88	49.2 ± 2.4
15	132	27.7 ± 3.0	132	54.0 ± 2.0
20	176	33.9 ± 3.8	176	68.3 ± 3.3

The results shown in Table 2 indicate that for either kind of surface finishing, the amount of silver increases with the number of cycles likewise, when the amount deposited on each of the composite electrodes was compared, it became clear that the ECPA gained a 100 % deposit as compared to the ECPL and this is due to the different roughness at the composite.

3.2.2. Effect of the potential scan rate on the silver deposition

Based on the results obtained through variation of the cycle number, it became important to produce CV programs at 20 cycles reducing silver onto both ECPL and ECPA electrodes within the -0.080 to -0.500 V range varying the potential scan rate; subsequently, the oxidation of silver was performed.

The results on the amount of silver deposited as a function of the potential scan rate are presented in Table 3.

Table 3. Amount of deposited silver as a function of the potential scan rate, after 20 cycles were applied within the -0.080 to -0.500 V reduction potential interval.

Deposition potential scan rate / Vs^{-1}	ECPL	ECPA
	Silver amount / nmoles	Silver amount / nmoles
0.010	187.5 ± 6.2	249.0 ± 5.2
0.020	94.4 ± 5.1	135.0 ± 4.2
0.050	42.5 ± 19.4	86.9 ± 14.1
0.100	33.9 ± 3.8	68.3 ± 3.3
0.150	16.3 ± 3.4	43.8 ± 2.2

The results presented in Table 3 indicate that at scan rates of 0.010 Vs^{-1} the amount of silver obtained on the surface of the composite used was larger than at 0.150 Vs^{-1} , although this amount was greater for the ECPA electrodes as compared with the ECPL. It is fair to state as preliminary conclusion from the potentiodynamic study, that the amount of silver deposited either on the ECPL or the ECPA increases with the cycle number and when the scan rate was small. Further, analysis of the CV results indicate that the amount of silver deposited was greater using the finer polishing of the ECPA composite, due to its increased surface area, that most likely provided a greater amount of nucleation and growth active sites, a fact that was considered when undertaking the potentiostatic study.

3.3. Potentiostatic silver electrodeposition study

Some of the potentiodynamic characteristics of silver electrodeposition have been proved so far, giving a metal coating on the ECPL and the ECPA, but it would be fitting to elucidate further through potentiostatic experiments the kinetics of the process, leading to the relevant nucleation and growth mechanism, and to add morphological relevant features of the resulting films as part of the characterization; thus the mechanism of silver nucleation onto ECPL and ECPA was studied.

3.3.1. Study on the silver nucleation mechanism

In order to find out about the silver nucleation and growth mechanism on the composites, studies were performed at different reduction potentials through chronoamperometry. The potentials were selected from the results obtained during cyclic voltammetry. To know the silver nucleation

mechanism it was necessary to analyze the non-dimensional plots $\left(\frac{j}{j_m}\right)^2$ vs $\left(\frac{t}{t_m}\right)$ obtained by substituting the co-ordinates of local experimental maxima at (t_m, j_m) . The results obtained were compared with theoretical 3D diffusion-limited models as described by Scharifker and Hills [27], where two limit cases are considered, high and low nucleation rate. At a high rate all nuclei are immediately formed with their number remaining constant throughout a short-lived process, giving thus rise to the so-called instantaneous nucleation and the current density is described by equation (1):

Instantaneous nucleation

$$\frac{j}{j_m}^2 = \frac{1.9542}{\left(\frac{t}{t_m}\right)} \left\{ 1 - \exp \left[-1.2564 \left(\frac{t}{t_m} \right) \right] \right\}^2 \quad (1)$$

On the other hand, when the nucleation rate is low, the nuclei form at progressively different times after one another during the electrochemical development at the surface, such that a progressive state of affairs controls time-formation of a metal deposit, which is described by equation (2):

Progressive nucleation:

$$\frac{j^2}{j_m^2} = \frac{1.2254}{\left(\frac{t}{t_m}\right)} \left\{ 1 - \exp \left[-2.3367 \left(\frac{t}{t_m} \right)^2 \right] \right\}^2 \quad (2)$$

Considering the geometric area on the ECPL and ECPA, an analysis was carried out of the plots $\left(\frac{j}{j_m}\right)^2$ vs $\left(\frac{t}{t_m}\right)$ based on the theoretical models mentioned, resulting that for both types of surfaces a tendency toward instantaneous nucleation became apparent, with diffusion-controlled 3D growth processes being in charge of the formation of the silver deposit, which are expected characteristics associated to a case of metal deposition.

In agreement with the estimations made by the Scharifker and Hills [27], it is known that when instantaneous nucleation occurs, N is equal to N_0 , and can be estimated through the following expression:

$$j_m = 0.6382 z F D c (kN)^{1/2} \quad (3)$$

Where D is the diffusion coefficient $\text{cm}^2 \text{s}^{-1}$, that is estimated through:

$$j_m^2 t_m = 0.1629 D (zFc)^2 \tag{4}$$

and

$$k = (8\pi cM / \rho)^{1/2}$$

where $M=107.86 \text{ gmol}^{-1}$, $c=2 \times 10^{-3} \text{ molL}^{-1}$ and

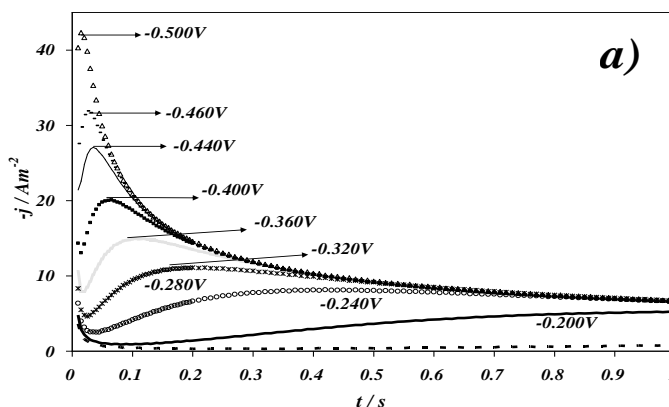
$$\rho = 10500 \text{ gdm}^{-3}$$

With the data obtained and equations (3) and (4) it is possible to evaluate D and N ; the results obtained are shown in Table 4.

Table 4. Estimations of the parameters D and N obtained for the 3D instantaneous nucleation on the ECPL and ECPA considering the geometric area of the electrodes.

ECPL					ECPA				
E_{dep}/V	j_m/Am^{-2}	t_m/s	$10^{-5}D/\text{cm}^2\text{s}^{-1}$	$10^{-15}N/\text{cm}^{-2}$	E_{dep}/V	j_m/Am^{-2}	t_m/s	$10^{-5}D/\text{cm}^2\text{s}^{-1}$	$10^{-15}N/\text{cm}^{-2}$
-0.200	4.3	1.55	4.73	2.54	-0.200	7.7	0.85	8.31	8.13
-0.320	12.8	0.2	5.40	22.5	-0.320	17.3	0.17	8.53	41
-0.500	48.9	0.015	5.91	328	-0.500	72.3	0.01	8.61	717

The results shown in Table 4 indicate that the nuclei density was greater for the ECPA as compared to the value estimated for its counterpart ECPL, which is agreement with current densities obtained, although if one observes the D values for both substrates used, there were differences, which are ascribed to the use of a nominal value of the areas during calculation of the current densities, rather than using the active areas for both substrates.



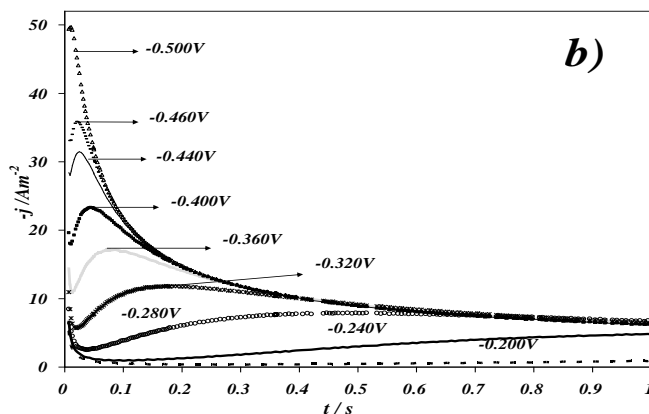


Figure 2. Families of experimental potentiostatic current transients obtained during silver electrodeposition onto composite electrodes a) ECPL and b) ECPA, in the system containing an aqueous AgNO_3 2 mM solution. The applied potentials are shown in the Figure.

Therefore, the diffusion coefficient used was that for the Ag^+ ion: $2.6 \times 10^{-5} \text{ cm}^2\text{s}^{-1}$ as given by Oliveira and Barbosa [33]. Once the corresponding calculations were obtained, it was found that the active areas were $4.43 \times 10^{-5} \text{ m}^2$ for the ECPA and $3.49 \times 10^{-5} \text{ m}^2$ for ECPL, respectively. With these results a new analysis of the nucleation and growth mechanism was carried out. The experimental potentiostatic current transients obtained during silver electrodeposition on the composite electrodes are shown in Figure 2 a) ECPL and b) ECPA.

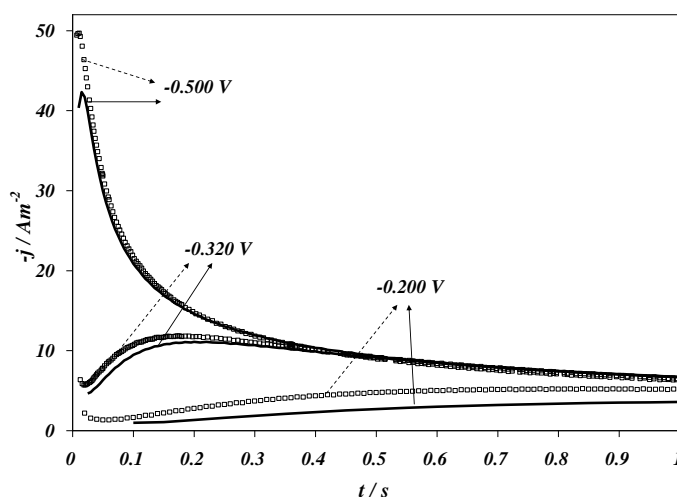


Figure 3. Comparison of the experimental potentiostatic current transients obtained during silver electrodeposition onto the ECPL (solid line), and the ECPA (symbols), at the potential shown in the Figure. Both systems containing aqueous AgNO_3 2 mM solution.

Figure 2 shows the experimental potentiostatic current transients obtained after applying the silver reduction potentials indicated therein: both transients' families exhibit current density increases

as a function of elapsing time, passing through a maximum at j_m at the corresponding t_m . Comparing the results obtained for both the ECPL and the ECPA, as shown in Figure 3, it can be observed that the j from the ECPA are larger compared to those from the ECPL and that the times at which the currents remain steady are almost the same for both cases, as shown in Table 5. Based on these results, the analysis of the potentiostatic current transients permitted to derive the nucleation and growth rate-controlling mechanism on the composites.

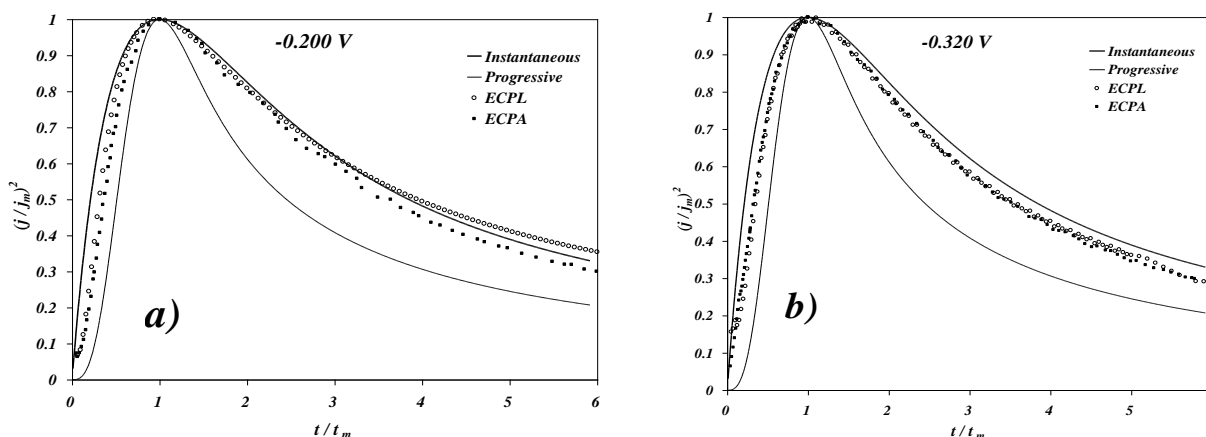
Table 5. Characteristics of the potentiostatic current transients of the ECPL and ECPA at the potentials indicated: -0.200, -0.320 and -0.500 V.

	ECPL			ECPA		
E applied / V	-0.200	-0.320	-0.500	-0.200	-0.320	-0.500
j_m / Am^{-2}	3.7	11.1	42.4	5.2	11.8	49.7
t_m / s	1.55	0.20	0.02	0.85	0.17	0.01

With the results from the active area determined for the composites and the data experimentally obtained an analysis was carried out based on the theoretical models described by the plots $\left(\frac{j}{j_m}\right)^2$ vs $\left(\frac{t}{t_m}\right)$. The latter are shown in Figure 4 for the potentials indicated: a) -0.200, b) -0.320 and c) -0.500V.

Even when the nucleation and growth mechanism does not change when performing the analysis based on the active areas of each composite, we now use equation (3) and consider the instantaneous nucleation to estimate the number density of active sites N_0 (cm^{-2}). The saturation number density of nuclei N_s (cm^{-2}) was evaluating according to (equation 5) proposed by Abyaneh [35], Isaev [36] and used by Zapryanova [37]. The results are shown in Table 6.

$$N_s = \frac{3.725z^2F^2}{\pi V_M j_m t_m} \tag{5}$$



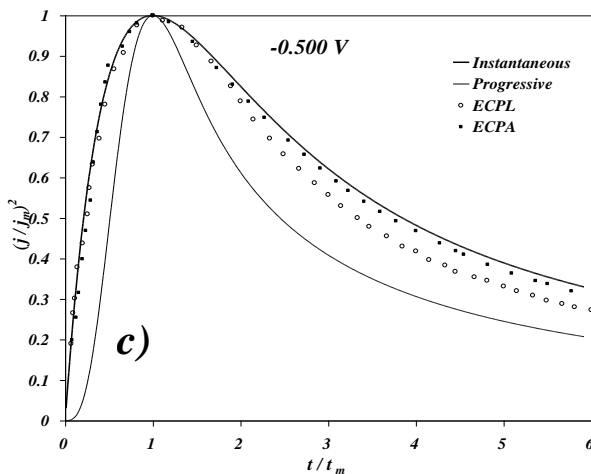


Figure 4. Non-dimensional plots of the current transients of the silver electrodeposition process on the composites a) -0.200V , b) -0.320V and c) -0.500V for ECPL and ECPA and the instantaneous and progressive theoretical models.

Table 6. Number density of active sites $N_0 (\text{cm}^{-2})$ and the saturation number density of nuclei $N_s (\text{cm}^{-2})$ for the potentials of -0.200 , -0.320 and -0.500V using the ECPL and ECPA composites considering the active area of the electrodes.

	ECPL			ECPA		
E applied/V	-0.200	-0.320	-0.500	-0.200	-0.320	-0.500
$10^{-15} N_0 / \text{cm}^{-2}$	1.88	16.9	247	3.71	19.1	339
$10^{-14} N_s / \text{cm}^{-2}$	3.18	19.2	258.8	5.35	26.0	250.1

When comparing the number density of active sites at different potentials on the same type of electrode and between the two electrodes, it can be observed that the amount of silver deposited will be different, which is why it becomes necessary to study the effect of potential and of deposition time on the amount of deposit on the ECPL and the ECPA.

3.3.2. Effect of potential and deposition time on the amount of silver deposited on the ECPL and ECPA

Once the silver nucleation mechanism onto the composites ECPL and ECPA has been studied, further experiments on silver deposition were carried out onto the said electrodes with two chosen potentials, -0.500 and -0.200V . These potentials were applied for various time periods to observe the response on the amount of metal deposited onto each composite. After $\text{Ag}(0)$ deposition, the metal deposits were oxidized for the same periods as those used in the potentiodynamic studies. Table 7

shows the results obtained on the amounts of silver deposited under the potentials chosen for different periods of time.

Table 7. Amount of deposited silver as a function of time for the two different potentials -0.500 and -0.200 V applied.

t / min	ECPL		ECPA	
	Silver amount / nmol -0.500 V	Silver amount / nmol -0.200 V	Silver amount / nmol -0.500 V	Silver amount / nmol -0.200 V
3.2	34.6 ± 2.0	58.3 ± 3.9	86.2 ± 1.7	103.6 ± 5.4
6.4	88 ± 20	100 ± 12	112 ± 20	136.8 ± 2.8
19.2	121 ± 14	149 ± 12	115 ± 12	280 ± 11
25.6	139 ± 18	184 ± 17	226 ± 18	375 ± 10
32	138 ± 21	244.1 ± 5.2	220 ± 17	497.4 ± 3.1

From the results shown in Table 7, it can be observed that for any deposition time the amount of silver deposited at -0.200 V was greater than at -0.500 V; although as is shown in Table 6, at -0.500 V, N_s is greater than a -0.200 V. However, these results are explained by the observations done during the experimentation where, a solid phase was found at the bottom of the flask (electrochemical cell). In this way, the application of a larger amount of energy to produce the electrodeposit, produce that the silver deposited began to come loose from the composite surface, a fact that was observable through the working cell and could be verified after deposition at -0.500 V for either the ECPL or the ECPA.

Furthermore, at -0.500 V there is a time where the amount of deposited silver does not longer increase, whereas at the less negative potential -0.200 V the amount of silver increased with deposition time. Likewise, it can be observed that the deposit was greater on the ECPA as compared with the other composite electrode ECPL, which is in agreement with the previous potentiodynamic results, also attributable to a greater surface area to effect metal deposition of the ECPA.

Furthermore the number nuclei was determined microscopically by SEM (scanning electron microscopy [40]) after 32 minutes of silver electrodeposition; the value obtained by SEM onto ECPL electrodeposited at -0.2 V ($N_{-0.2V} = 1 \times 10^{13}$ nuclei cm^{-2}) is one order of magnitude lower than the N_s estimated at the ECPL and at the same potential ($N_{s -0.2V} = 3.18 \times 10^{14}$ nuclei cm^{-2}), this result supports the fact that silver deposited begins to come loose from the composite surface. Nevertheless the results are in good agreement between the experimental data and the N_s for instantaneous nucleation.

Figure 5 shows the silver crystals electrodeposited on a ECPL electrode at $E = -0.200$ V using different magnifications. From these images one could clearly noted that silver deposition actually occurs over most of the electrode surface by multiple nucleation of hemispheres as the theoretical model used for the analysis of the current transients required.

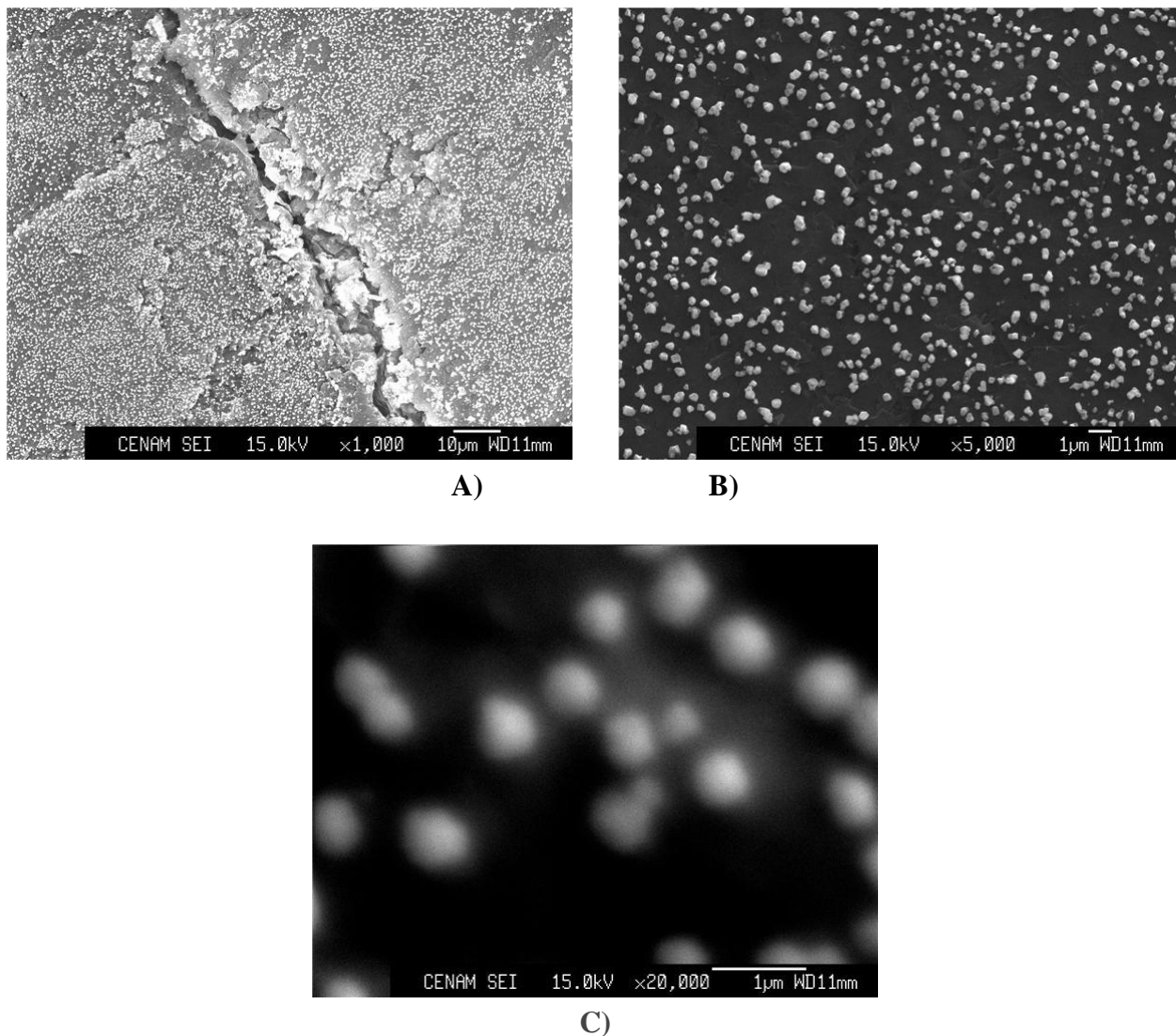


Figure 5. Silver crystals electrodeposited on a ECPL electrode at $E=-0.200V$. Magnifications are: a) x 1,000, b) x 5,000, and c) x 20,000.

4. CONCLUSIONS

It has been observed that the amount of potentiodynamically deposited silver depended on the surface rugosity of the composites having two different surface finishes, a fact which is in agreement with the results of Sosa et al [34], for the electrodeposition of lead onto glassy carbon electrode with various induced rugosity, although the most significant difference is that for silver, the rate controlling 3D nucleation and growth process was instantaneous and limited by the diffusion of $Ag(I)$ ions, regardless of the surface condition of the receiving substrate. The comparison of the amount of silver deposited through both methods indicated that this is larger when deposition was effected potentiostatically onto the composites finished with alumina $1\ \mu m$ ECPA. In another hand, the amount of silver increase with the time; nonetheless, this is not infinite since silver deposited begins to come

loose from the composite surface at the tree potentials since the beginning. Nevertheless, the results obtained will be used to optimize the construction parameters of composite electrodes with a silver chloride coating [41] to function as an efficient working alternative for *screen-printing* electrodes and *PLD* in the *thick-film* and *thin-film* technologies.

ACKNOWLEDGMENT

G.V.R acknowledges Consejo Nacional de Ciencia y Tecnología (CONACYT) for the studentship granted through number 184923 and to Red ALFA II for the *BioSenIntg* Clave: II-0486-FCFA-FCD-FI. MPP thank CONACyT for support through projects 82932 and 24658 (“Nucleación y crecimiento electroquímico de nuevas fases”). Also M.R.R., M.P.P. and M.T.R.S. gratefully thank the SNI for the distinction of their membership and the stipend received. MTRS thanks CONACyT for support through project 82932. MEPP and MARR wish to thank the Departamento de Materiales, UAM-A, for the financial support given through projects 2261203, 2261204 and 2261205 and PROMEP for support give to RED SIATA

References

1. J. Ives, J. Janz, *Reference Electrodes*, Academic Press, New York (1961).
2. D Jr. Caton, *J. Chem. Educ.*, 12 (1973) A571
3. C. Galán-Vidal, J. Muñoz, S. Alegret et al, *Sens. Actuators B*, 45 (1997) 55
4. H. Suzuki, H. Shiroishi, S. Sasaki et al, *Anal. Chem.*, 71 (1999) 5069
5. D. Desmond, B. Lane, J. Alderman et al, *Sens. Actuators B*, 44 (1997) 389
6. K. Eine, S. Kjelstrup, K. Nagy et al *Sens. Actuators B*, 44 (1997) 381
7. A.Simonis, T. Krings, H. Lüth et al, *Sensors*, 1 (2001) 183
8. J. Pedrotti, L. Angnes, I. Gutz, *Electroanalysis*, 7 (1996) 673
9. H. Suzuki, H. Shiroishi, S. Sasaki et al, *Sens. Actuators B*, 46: (1998) 104
10. H. Suzuki, H. Shiroishi, S. Sasaki et al, *Sens. Actuators B*, 46 (1998)146
11. T. Matsumoto, A. Ohashi, N. Ito, *Anal. Chim. Acta*, 462 (2002)253
12. L. Tymecki, E. Zwierkowska, R. Koncki, *Anal. Chim. Acta*, 526 (2004) 3
13. H. Kim, Y. Kim, B. Kang, *Sens. Actuators B*, 97 (2004) 348
14. A.Simonis, H. Lüth, J. Wang et al, *Sens Actuators B*, 103 (2004) 429
15. J. Costa Alambra (ed) *Fundamentos de Electrónica*, primera edición, España (1981)
16. D. Manning, *Talanta*, 10 (1963) 255
17. J. Golas, J. Osteryoung, *Anal. Chim. Acta*, 192 (1987) 225
18. B. Costa, J. Canulo, A. Arvia, *J. Electroanal. Chem.*, 244 (1988) 261
19. D. Alonzo, B. Scharikfer, *J. Electroanal. Chem.*, 274 (1989) 167
20. M. Martins, R. Salvarezza, A. Arvia, *Electrochim. Acta*, 36 (1991) 1617
21. J. Rodríguez, D. Taylor, H. Abruña, *Electrochim. Acta*, 38 (1993) 235
22. K. Márquez, G. Staikov, J. Schultze, *Electrochim. Acta*, 48 (2003) 875
23. M. Miranda-Hernández, I. Gonzalez, *Electrochim. Acta*, 42 (1997) 2295
24. G. Ramírez, S. Alegret, R. Céspedes et al, *Anal. Chem.*, 6 (2004) 503
25. G. Álvarez-Romero, A. Rojas-Hernández, A. Morales-Pérez et al, *Biosens. Bioelectronics*, 19 (2004)1057
26. S. Alegret, F. Céspedes, D. Matorrel et al, *Biosens. Bioelectronics*, 11 (1996) 35
27. B. Scharikfer, G. Hills, *Electrochim. Acta*, 28 (1983) 879
28. B. Scharikfer, J. Mostany, *J. Electroanal. Chem.*, 177 (1984) 13
29. L. Heerman, A. Trallo, *J. Electroanal. Chem.*, 470 (1999) 70

30. L. Mendoza-Huizar, J. Robles, M. Palomar-Parvavé, *J. Electroanal. Chem.*, 521 (2002) 95
31. L. Mendoza-Huizar, J. Robles, M. Palomar-Parvavé, *J. Electroanal. Chem.*, 545 (2003) 39
32. O. Brylev, L. Roué, D. Bélanger et al, *J. Electroanal. Chem.*, 581 (2005) 22
33. G. De Oliveira, L. Barbosa et al, *J. Electroanal. Chem.*, 578 (2005)151
34. E. Sosa, G. Carreño et al, *Appl. Surf. Sci.*, 153 (2000) 245
35. M. Y. Abyaneh, *Electrochim. Acta*, 27 (1982)1329
36. V. Isaev, J. Baraboshkin, *J. Electroanal. Chem.*, 377 (1994) 33
37. T. Zapryanova, A. Hrussanova, A. Milchev, *J. Electroanal. Chem.*, 600 (2007) 311
38. M. R. Majidi, K. Asadpour-Zeynali, B. Hafezi, *Int. J. Electrochem. Sci.*, 6 (2011) 162
39. A.I. Inamdar, S. H. Mujawar, P. S. Patil, *Int. J. Electrochem. Sci.*, 2 (2007) 797
40. Lj. J. Pavlović, M. M. Pavlović, M. G. Pavlović, N. D. Nikolić, M.V. Tomić, *Int. J. Electrochem. Sci.*, 5 (2010) 1898 – 1910
41. H.H. Hassan, M. A. M. Ibrahim, S. S. Abd El Rehim, M. A. Amin, *Int. J. Electrochem. Sci.*, 5 (2010) 278 – 294